

# Transport and Separation of Biomolecular Cargo on Paramagnetic Colloidal Particles in a Magnetic Ratchet

Pietro Tierno,<sup>\*,†</sup> Sathavaram V. Reddy,<sup>†</sup> Michael G. Roper,<sup>†</sup> Tom H. Johansen,<sup>§</sup> and Thomas M. Fischer<sup>\*,||</sup>

*Department of Chemistry and Biochemistry, Florida State University, Tallahassee, Florida 32306-4390, Departament de Química Física, Universitat de Barcelona, Martí i Franquès 1, 08028 Barcelona, Spain, Department of Physics, University of Oslo, P.O. Box 1048, Blindern, Norway, and Institut für Experimentalphysik V, Universität Bayreuth, 95440 Bayreuth, Germany*

*Received: November 5, 2007; In Final Form: December 17, 2007*

Paramagnetic particles in a magnetic ratchet potential were transported in discrete steps in an aqueous solution on the surface of a magnetic garnet film. The proposed technique allows the simultaneously controlled, dispersion-free movement of an ensemble of paramagnetic particles across the surface. External magnetic modulations were used to transport the particles in a defined direction, and a current reversal upon changing the size of the particles was used to separate particles having different diameters. Doublets consisting of a larger and a smaller particle functionalized with complimentary oligonucleotides and bound via Watson–Crick base pairing were separated after melting the double stranded DNA.

## Introduction

Transport is an essential nonequilibrium feature equally important for life and for technological applications. A rich variety of transport processes in one, two, and three dimensions and on multiple scales exists that are well-adapted for the specific purposes they serve. On the micro- and nanoscale, major effort has been devoted to the controlled manipulation of colloidal particles with specific surface functionalities that bind or release chemical or biochemical cargo of complementary functionalities.

Upon miniaturization, fluctuations in the environment increase the difficulty of transport in a controlled way. One way of outsmarting fluctuations that tend to randomize the motion is via the ratchet effect.<sup>1</sup> A Brownian ratchet is a device that converts the deviation of the fluctuations from thermal equilibrium into directed motion. Key elements of a pulsating ratchet are a potential that fluctuates in time such that particles part of the time are entrapped within the wells and part of the time are free to diffuse across the barriers separating those wells. An asymmetry in the potential then creates a preference for the motion in one direction.

As a consequence, one way to realize transport on a colloidal scale is, for example, to induce a ratchet effect at a solid/liquid interface. The ratchet requires a gradient or surface structure interacting with the overlying colloids. Uses of external optical or magnetic fields represent the most promising option for colloidal manipulation. Magnetic fields are preferred in some cases because they do not interact with biological matter.

Colloidal particles that can be easily manipulated with external magnetic fields are paramagnetic particles, made by a polymer matrix and doped with superparamagnetic magnetite grains.<sup>2</sup> The major advantage in using these particles is that

their surface can be functionalized to bind and transport a specific molecule that could then be used, for example, to produce readable/writable memory devices. Thus, several transport techniques have been developed by using various miniaturized devices such as microchannel, microcoils, or special patterned substrates.<sup>3,4</sup> In most cases, such devices allow programmable motion of only one particle or of a small cluster of nonseparable particles. To realize simultaneous control over a large ensemble of paramagnetic particles, one should use magnetic fields with a spatial variation on the colloidal scale.

Heterogeneous magnetic fields on a colloidal scale can be created in different ways. Friedmann et al.<sup>5,6</sup> used lithographic deposition of cobalt cylinders to form ferromagnetic micropatterns. Gunnarson et al.<sup>7</sup> deposited a permalloy into elliptical island patterns and showed their ability to transport paramagnetic particles along the ellipses. Magnetic ferrite garnet films also can be used to produce magnetic heterogeneities.<sup>8</sup> These heterogeneities are self-assembled magnetic domain patterns that can be altered in shape and size with external homogeneous magnetic fields. In this way, one can realize a rich variety of a particle's transport mode for a large assembly of colloidal particles, with individual control over each particle.

Here, we discovered a magnetic colloidal ratchet with a discrete time base that allows programmable, dispersion-free motion of an ensemble of paramagnetic particles. This was achieved by placing the paramagnetic particles on top of the surface of a ferrite garnet film with a magnetic domain pattern forming a periodic array of stripes with magnetization alternating up and down. In the absence of external magnetic fields, the paramagnetic particles were trapped above the domain walls, and the system therefore represents a nonvolatile form of discrete data storage. By applying simple time-dependent magnetic field pulses, the whole assembly of particles can be shifted by one period of the magnetic domain pattern. In this way, biomolecules attached to the particles can be addressed and set to move sequentially into a desired location where they are analyzed.<sup>9</sup> Since the motion is discrete (one magnetic period per pulse),

\* Corresponding author. E-mail: thomas.fischer@uni-bayreuth.de.

<sup>†</sup> Florida State University.

<sup>‡</sup> Universitat de Barcelona.

<sup>§</sup> University of Oslo.

<sup>||</sup> Universität Bayreuth.

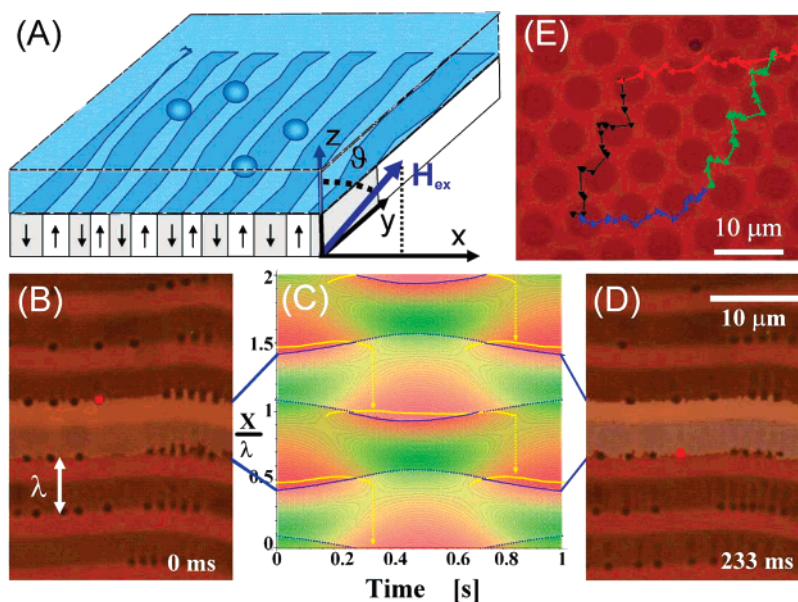


**Figure 1.** (A) Scheme of a uni-axial ferrimagnetic garnet film with an aqueous solution containing paramagnetic particles. The external magnetic field  $H_{\text{ext}}$  oscillates in the  $(x,z)$ -plane with an inclination  $\theta$ . (B and D) Polarization microscope images showing the motion of paramagnetic particles on top of parallel stripes of wavelength  $\lambda$ . To guide the eye, one particle is marked in red and two stripes are in white. (C) Color coded potential energy landscape (low energies in red and high energies in green) of a particle residing at height  $z = a = 0.1 \lambda$  as a function of the particle position and time. The blue lines indicate the periodic modulation of the domain wall position. The minimum energy positions at a given time follow the yellow lines. (E) Two-dimensional trajectory of a particle on a film having a magnetic bubble domain pattern. Videos are included in the Supporting Information.

the order of the particles is conserved (i.e., there is no dispersion and no loss of data).

### Experimental Procedures

As a platform for particle motion, we used ferrite garnet films of the composition  $\text{Y}_{2.5}\text{Bi}_{0.5}\text{Fe}_{5-q}\text{Ga}_q\text{O}_{12}$  ( $q = 0.5-1$ ) (Figure 1A), which were epitaxially grown on a gadolinium gallium garnet substrate, resulting in ferrimagnetic films with a uniaxial anisotropy. The films that typically had a thickness of  $4 \mu\text{m}$ , and a spontaneous magnetization with magnitude  $M_s = 1.7 \times 10^4 \text{ A/m}$ , formed a periodic magnetic domain pattern with wavelength  $\lambda = 10.9 \mu\text{m}$ . The pattern can be observed directly in a polarizing microscope due to the large Faraday effect in these optically transparent garnets. As a carrier of the biomolecular information, we used paramagnetic polystyrene particles having different sizes ( $1.0$  and  $2.8 \mu\text{m}$  in diameter) and surface compositions (carboxylic and streptavidin). The particles are paramagnetic due to the presence of superparamagnetic grains inside the polymer matrix (Dynabeads, Dynal). An aqueous suspension of the particles ( $\sim 10^7$  beads/mL) was deposited on top of the garnet film, and after a few minutes, the particles were observed to sediment on the surface of the film. To prevent the particles from sticking to the surface, the garnet film was coated with a thin layer of polysodium 4-styrene sulfonate.<sup>10</sup> Polarization microscopy and fast video recording were used to visualize the dynamics of both the particles and the stripe domains in the garnet film.<sup>11</sup> The external magnetic field was provided by two coils with the main axes along the  $(x,z)$ -directions. The coils were connected to an amplifier being fed by a wave generator and were able to produce a homogeneous magnetic field up to  $H = \sim 0.5 \times 10^5 \text{ A/m}$  in each direction above the sample area.

**Realization of DNA-Linked Asymmetric Doublets.** The DNA linkage was realized by using two single strand sequences: 5'-/5Bio/TCA CTC AGT ACG ATA TGC GGC ACA G-3' on the small particles and the complimentary sequence

5'-/5Bio/CTG TGC CGC ATA TCG TAC TGA GTG A-3' on the large particles (IDT Technologies, Inc.). The particles were washed and re-dispersed in two separate individual batches made with a  $20 \text{ mM NaCl}$  buffer solution ( $\text{pH } 8.0$ ) at a concentration of  $\sim 10^7$  beads/mL. A total of  $6 \mu\text{L}$  of a single stranded DNA solution containing one of the two sequences was then added to the corresponding batch. Prior to mixing, the particles were allowed to equilibrate for 30 min. Then, the batches were mixed and placed in a spatially homogeneous magnetic field ( $\sim 0.5 \text{ T}$ ) for 15 min. The field aligned the particle into chains and thus promoted the linkage between the DNA strands.

### Results and Discussion

**Discrete Transport of Paramagnetic Particles.** Figure 1A shows a scheme of the uni-axial garnet film that in the absence of an external magnetic field assembled into parallel and equally sized alternate upward and downward magnetized ferrimagnetic domains. A magnetic stray field,  $H$ , above the film was generated from the domain walls and points in the positive (negative)  $z$ -direction above the upward (downward) magnetized domains and into the positive (negative)  $x$ -direction above the domain walls. A paramagnetic particle of volume  $V$  and susceptibility  $\chi$  placed in this field acquired a magnetic moment  $m = V\chi H$  pointing in the field direction and had the potential energy  $U = -\mu_0 m H = -\chi H^2$ . Thus, when no external field was applied, the particles were pinned at the domain wall positions. External magnetic fields  $H_z^{\text{ext}}$  normal to the garnet film strengthened the field above the domains magnetized parallel to the field and weakened the field of the antiparallel domains. In plane components of the external field  $H_{\text{ext}}$  strengthen and weaken the fields above the alternating domain walls. Paramagnetic particles dispersed in an aqueous solution on top of the garnet film were attracted toward the domain walls where the field is maximal. A sinusoidal external field modulation with both in-plane and normal components let the domain walls alternate between strong and weak and the domains alternate between being a majority and being a minority domain. The

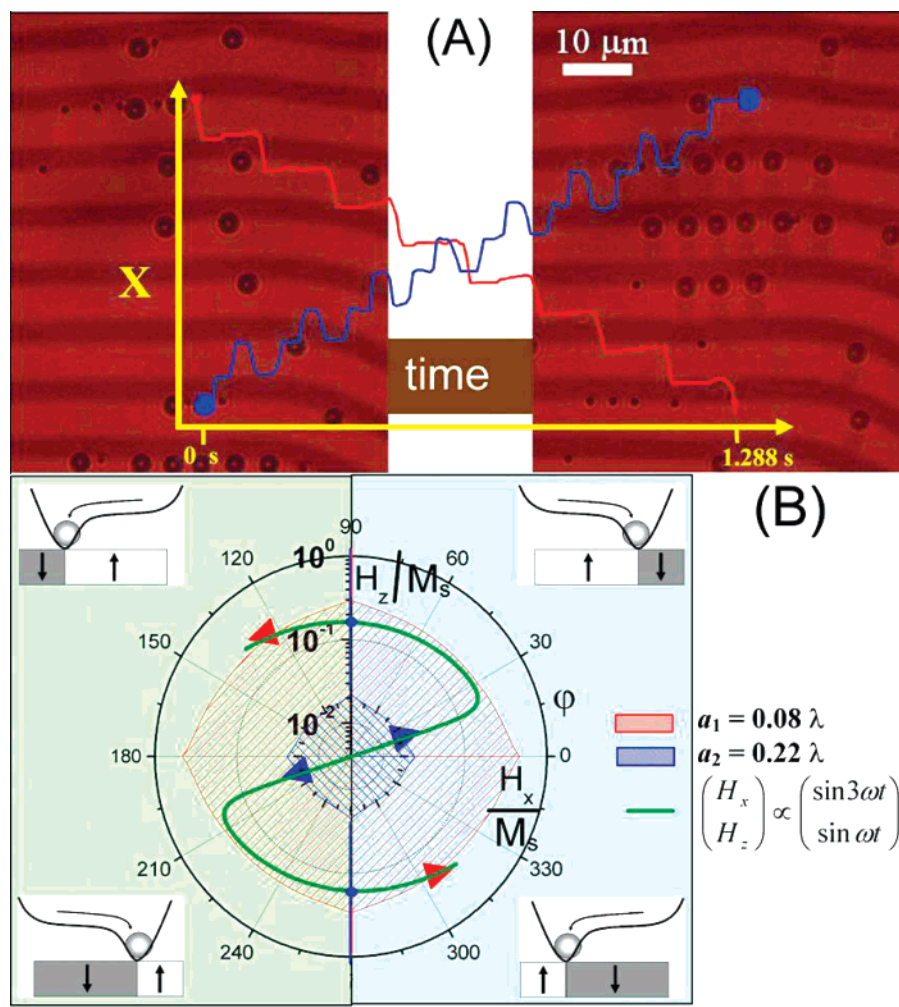


**Figure 2.** (A) Polarization microscope images of a garnet film with small ( $a_1 = 0.08 \lambda$ , red) and large ( $a_2 = 0.22 \lambda$ , blue) particles. Trajectories of both particles are superimposed. The motion occurs in discrete steps that lead to a net motion in opposite directions separating the particles. Video is included in the Supporting Information. (B) Separation mechanism: The external magnetic field modulations occur along the green line. The discrete hopping of the large (small) particles occurs above the blue (red) thresholds. Hopping directions are indicated by small schemes in each quadrant.

potential energy minimum for the paramagnetic particles (yellow lines in Figure 1c) was at the strong domain walls (solid blue lines in Figure 1c). During the modulation, a previously stable position of a particle at a strong wall will first switch to being metastable when the domain wall becomes weak (dotted blue line in Figure 1c) and then turn unstable when the destabilizing in-plane field surmounts a specific threshold. Above the threshold, the particle will then hop to a neighboring strong domain wall via the majority domain (yellow arrows in Figure 1c). Hence, the direction of hopping is controlled by the normal component of the external magnetic field. The hopping in the opposite direction is suppressed because the magnetic field above the minority domain is weak that the particle prefers to hop via the higher magnetic field of the majority domain to the new strong domain wall.

In Figure 1B,D are two polarization microscope images showing the motion of paramagnetic particles on top of the garnet film when the simplest asymmetric fluctuation is applied (i.e., a periodic magnetic field of intensity  $H_0 = 1.3 \times 10^4$  A/m, inclination  $\vartheta = 51^\circ$ , and angular frequency  $\Omega = 18.8$  s $^{-1}$ ). The particle marked red in Figure 1B is pinned to one domain wall at  $t = 0$ . Figure 1C shows the color coded energy landscape<sup>12</sup> (low energies in red and high energies in green) of the particle as a function of the particle position and time. The time-dependent positions of the domain walls are shown as blue lines

in Figure 1C. The domain walls are strong in the period indicated by solid lines and weak when dotted in Figure 1C. The minimum energy position at a given time follows the yellow lines in Figure 1C that lie close to the strong walls, and the particles hop to the closest domain wall (yellow arrows in Figure 1C) when the potential energy minima change to a saddle point  $\partial U/\partial x = \partial^2 U/\partial x^2 = 0$  as the external magnetic field reaches the threshold value. During one period, the particles hop twice and advance by one wavelength as shown in Figure 1D at  $t = 233$  ms. The advantage of using the garnet film as a source of magnetic background potential is that the domain wall motion is essentially free from intermittent behavior and hysteresis. This makes the cyclic displacements and the device performance fully reversible. Moreover, we demonstrate that the motion control is not limited to one dimension as shown in Figure 1E. Using magnetic bubble domains instead of stripe domains extends all capabilities discussed here to a full two-dimensional control.<sup>13</sup> Superimposed on the image is the trajectory of a paramagnetic particle that moves in different directions by the use of magnetic modulations that exploit all three space dimensions.

**Size-Dependent Separation of Two Paramagnetic Particles.** Our experiments and calculations show that the threshold magnetic field for the particle hopping depends on the distance of the particle center of mass from the domain wall. The domain wall represents a singularity of the magnetic field, and the closer



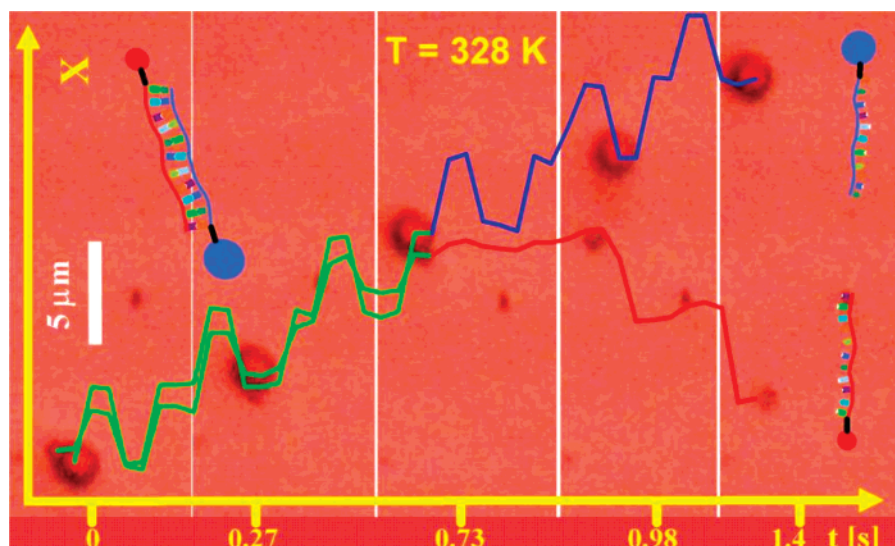


**Figure 3.** Polarization microscope sequence of a doublet linked via Watson–Crick base pairing of complementary DNA strands attached to the particles. The doublet discretely moves along the stripe pattern (green trajectory) until the DNA melts in the hot zone, and the two colloids unbind and move in opposite directions (red and blue trajectories). Video is included in the Supporting Information.

a particle may approach the singularity, the larger the trapping is. For this reason, it is easier to free the larger particles than to free the smaller particles. In Figure 2, we exploited this distinctive feature to separate and sort particles based on their size. Figure 2A shows two polarization microscopy images ( $t = 0$  and  $1.28$  s) of large and small particles trapped in the stripe pattern. We marked one large (diameter  $a_2 = 0.22 \lambda$ ) particle in blue and one small particle ( $a_1 = 0.08 \lambda$ ) in red and superimposed their trajectories on the two images (Figure 2A). Particle separation during motion was obtained by using a modulation of the form  $(H_x, H_z) = H_0 (\sin 3\Omega t, \sin \Omega t)$ , having the amplitude  $H_0 = 8500$  A/m and angular frequency  $\Omega = 18.8$  s $^{-1}$ , where the in-plane component oscillates with triple the frequency of the normal component. As a result, the external magnetic field points to different directions when it surmounts the threshold for freeing the large and the small particles. The magnetic modulation creates a motion where large particles hop thrice: twice in a forward and once in a backward direction (blue trajectory in Figure 2A), while small particles only hop one step backward (red trajectory in Figure 2A). After 8 field cycles, the magnetic carriers have exchanged positions. When accidental collisions occur between oppositely moving particles, the small particle slides over the surface of the large one and stays within the particle line as if no collision took place. Figure 2B shows the separation mechanism, where we plotted the metastable regions (blue and red shaded areas for the large and small particles) as a function of the in-plane and normal component of the external field. The external field modulation cycles back and forth along the green solid line in Figure 2B and hence points into different directions as it changes strength. Hopping directions and stable positions of the particles vary from one quadrant to the next as indicated by the small schemes. In the shaded region in Figure 2B, the position above the weak wall is metastable, and the position above the strong wall is stable. For fields exceeding the threshold, the position above the weak wall becomes unstable, and particles hop to the strong wall. No hopping occurs upon re-entering the shaded region. All particles remain in their stable position above the strong wall. The strong walls become weak, and the particle position becomes metastable when  $H_x$  changes sign. Only as the field surmounts the threshold with the opposite sign do the particles hop again. The large particles undergo two additional reversible

hops when the in-plane component changes sign twice above the threshold. We also found that more complex modulations  $(H_x, H_z) = H_0 (\sin 5\Omega t, \sin \Omega t)$  can be used to single out mid-sized particles (moving in the positive  $x$ -direction) from both larger and smaller particles (moving in the negative  $x$ -direction) at the same time. In this case, there are two current inversions as a function of bead size. The device can be understood as a ratchet driven by periodic external modulations. The sinusoidal form of the modulation is not essential; a fluctuating field having the same correlation between its strength and its orientation would result in the same sort of particle motion. It exhibits all features of a thermal ratchet such as current reversal.<sup>1</sup> Here, we used the current reversal for the separation of the particles.

#### Separation of Molten Complementary Oligonucleotides.

We used our method to effectively separate colloidal particles carrying complementary biomolecular information. We realized an asymmetric doublet by attaching complementary biotin labeled single strands of oligonucleotides onto streptavidin-coated particles with different sizes ( $1.0$  and  $2.8 \mu\text{m}$  in diameter). Watson–Crick base pairing between the complementary 25 base pair DNA strands provided a link between the differently sized particles that remained stable at ambient temperature. In Figure 3 are a series of microscope images that show the doublet motion and subsequent separation when the composite particle crosses a region heated<sup>14</sup> above the DNA melting temperature. Prior to entering the hot zone, the doublet was moved across the garnet surface (green trajectories in Figure 3) by using the field modulation method described in Figure 2. Once entering the hot zone, the doublet separated into individual particles with the large particle containing one strand of oligonucleotides and continuing the doublet motion (blue trajectory in Figure 3), while the small particle with the complementary strand reversed its direction (red trajectory in Figure 3).<sup>15,16</sup> Re-annealing of the two particles did not occur since the solution remained above the melting temperature of the DNA strands. The reversible character of the temperature induced DNA hybridization allows for programmable rupture and recombination of complementary DNA strands, similar to temperature cycles in polymerase chain reactions. The process shown in Figure 3 and its reverse are only an example of operations that can be performed with our device. On the basis of the strength of the DNA linkage between

different strands on the two particles, the result of a temperature change can be different (separation or no separation).

## Conclusion

We developed a method for the programmable discrete motion and separation of arrays of paramagnetic particles on tuneable parallel stripes of a magnetic garnet film. The particle motion is free of dispersion and was achieved by applying external modulated magnetic fields to an array of paramagnetic particles deposited on the garnet film. The proposed technique has the potential to improve and simplify already existing methods to transport colloidal particles that make use of more complicated microdevices. The realization of garnet films with smaller stripe periods is not a difficult task. Smaller stripe patterns would allow for further miniaturization. The singularity of the magnetic field near the wall is logarithmic and would help to prevent thermal fluctuations exceeding the magnetic trapping forces due to the closer approach of the smaller particles to the domain wall singularity. We expect the fluctuation to finally win over the magnetic heterogeneities somewhere in the nanometer range. By attaching specific molecules to individual paramagnetic particles, one can realize a magnetic shift register that allows for the storage and logical manipulation of biochemical information transported by the particles.

**Acknowledgment.** This material is based upon work supported by the National Science Foundation under CHE-0649427. T.H.J. thanks The Research Council of Norway for financial support.

**Supporting Information Available:** Movies S1 B–D, S1 E, S2, and S3. This material is available free of charge via the Internet at <http://pubs.acs.org>.

## References and Notes

- (1) Reimann, P. *Phys. Rep.* **2002**, *361*, 57.
- (2) Fonnum, G.; Johansson, C.; Molteberg, A.; Morup, S.; Aksnes, E. *J. Magn. Magn. Mater.* **2005**, *293*, 41.
- (3) Fan, Z. H.; Mangru, S.; Granzow, R.; Heaney, P.; Ho, W.; Dong, Q. P.; Kumar, R. *Anal. Chem.* **1999**, *71*, 4851.
- (4) Ueberfeld, J.; El-Difrawy, S. A.; Ramdhanie, K.; Ehrlich, D. J. *Anal. Chem.* **2006**, *78*, 3532.
- (5) Yellen, B.; Friedman, G.; Feinerman, A. *J. Appl. Phys.* **2003**, *393*, 7331.
- (6) Yellen, B.; Friedman, G.; Feinerman, A. *J. Appl. Phys.* **2002**, *91*, 8552.
- (7) Gunnarsson, K.; Roy, P. E.; Felton, S.; Pihl, J.; Svedlindh, P.; Berner, S.; Lidbaum, H.; Oscarsson, S. *Adv. Mater.* **2005**, *17*, 1730.
- (8) Helseth, L. E.; Wen, H. Z.; Hansen, R. W.; Johansen, T. H.; Heinig, P.; Fischer, T. M. *Langmuir* **2004**, *20*, 7323.
- (9) Gosse, C.; Croquette, V. *Biophys. J.* **2002**, *82*, 3314.
- (10) Decher, G. *Science (Washington DC, U.S.)* **1997**, *277*, 1232.
- (11) Tierno, P.; Muruganathan, R.; Fischer, T. M. *Phys. Rev. Lett.* **2007**, *98*, 28301.
- (12) An analytical expression for the internal energy of a striped garnet film has been provided in Tierno, P.; Reddy, S. V.; Johansen, T. H.; Fischer, T. M. *Phys. Rev. E: Stat., Nonlinear, Soft Matter Phys.* **2007**, *75*, 41404.
- (13) Tierno, P.; Johansen, T. H.; Fischer, T. M. *Phys. Rev. Lett.* **2007**, *99*, 38303.
- (14) The region was electrically heated from below.
- (15) According to nearest neighbor thermodynamics, the predicted melting temperature for the DNA sequence used in our experiment was 327 K in a 20 mM NaCl aqueous solution. Increasing the temperature at  $T = 327$  K does not disrupt the streptavidin–biotin bond, which remains stable at temperatures higher than 350 K. See ref 16.
- (16) Gonzalez, M.; Bagatolli, L. A.; Echabe, I.; Arrondo, J. L. R.; Argarana, C. E.; Cantor, C. R.; Fidelio, G. D. *J. Biol. Chem.* **1997**, *272*, 41.